



HAL
open science

First in situ tests of a new electrostatic resistivity meter

Sébastien Flageul, Michel Dabas, Julien Thiesson, Fayçal Rejiba, Alain Tabbagh

► **To cite this version:**

Sébastien Flageul, Michel Dabas, Julien Thiesson, Fayçal Rejiba, Alain Tabbagh. First in situ tests of a new electrostatic resistivity meter. *Near Surface Geophysics*, 2013, 11 (3), pp.265-273. 10.3997/1873-0604.2012063 . halshs-01513101

HAL Id: halshs-01513101

<https://shs.hal.science/halshs-01513101v1>

Submitted on 25 Apr 2017

HAL is a multi-disciplinary open access archive for the deposit and dissemination of scientific research documents, whether they are published or not. The documents may come from teaching and research institutions in France or abroad, or from public or private research centers.

L'archive ouverte pluridisciplinaire **HAL**, est destinée au dépôt et à la diffusion de documents scientifiques de niveau recherche, publiés ou non, émanant des établissements d'enseignement et de recherche français ou étrangers, des laboratoires publics ou privés.

1 **First *in situ* tests of a new electrostatic resistivity meter**

2 Sébastien Flageul¹, Michel Dabas², Julien Thiesson¹, Fayçal Rejiba¹ & Alain Tabbagh¹

3

4 ¹UMR Sisyphe, UPMC/CNRS, case 105, 4 place Jussieu 75252 Paris Cedex 05, France

5 ²GEOCARTA, 5 rue de la Banque 75002 Paris, France

6

7 **Abstract**

8 If field applications of the electrostatic method are limited to roughly the first ten
9 metres due to the necessity of staying in the low induction number domain, the possibilities it
10 opens in urban area surveying, dry hole resistivity logging, non-destructive testing and
11 laboratory studies of the complex resistivity justify the design of a new multi-frequency
12 resistivity meter presenting a very low input capacitance and a high phase sensitivity. After a
13 first series of sample measurements in laboratory, the new resistivity meter was tested in two
14 different field contexts: the mapping of building remains in a Gallo-roman archaeological site
15 under a flat meadow, and the assessment of the anthropogenic layers thickness in a town. The
16 first test allowed a direct comparison with previous galvanic resistivity measurements and
17 proved a very good agreement between both in magnitude and spatial distribution of electrical
18 resistivity. The second test established its reliable measuring abilities in a disturbed
19 environment.

20

21 **Key words:** electrical resistivity, electrostatic method, non galvanic capacitive contacts,
22 archaeological and engineering applications

23

24 **Introduction**

25 Electrical resistivity is a relevant parameter for near surface investigations as it
26 exhibits a very large range of variation and is highly dependent upon clay and water content

27 within earth materials. Since nearly over one century, a wide set of techniques were thus
28 developed for performing its measurement, among which the mostly used galvanic
29 measurements with a four electrode array can be considered as the reference technique.
30 Unfortunately galvanic contact is not possible over all surfaces. If electromagnetic induction
31 methods have also been applied, their ability to detect resistive targets remains limited.
32 Moreover, measurements are sensitive to the presence of metallic objects which limits their
33 use in difficult environments, like towns or waste disposals for example. E.M. induction
34 methods cannot also be used at laboratory scale for resistivity and permittivity determinations.
35 In electrostatic method, measurements are achieved without any galvanic contact by
36 electrostatic influence only (Grard and Tabbagh 1991, Tabbagh *et al.* 1993, Kuras *et al.*
37 2006). This opens the possibility to survey over insulating surfaces like tarmac, pebble stones,
38 concrete slabs, etc. and in magnetically and/or electromagnetically noisy environments.

39 The poles that are used both for current injection and voltage measurements
40 correspond to simple metallic pieces like for example a sheet of copper insulated with rubber.
41 The surface of the poles determines the capacitance and thus the impedance of the system. For
42 example a 20cm x 20cm metallic sheet has a 9pF capacitance in free air and 18pF when put
43 on the ground. The corresponding impedances being 9 M Ω at 1kHz and 90 k Ω at 100 kHz, it
44 is difficult to use frequencies lower than several kHz. Both this frequency constraint and the
45 application of the low induction number condition (Benderitter *et al.* 1994) limit the size of
46 the arrays and thus the depth of investigation to roughly the first ten metres.

47 Despite this depth limitation, its applications cover a large range from soundings in
48 both field and urban contexts (Benderitter *et al.* 1994, Tabbagh and Panissod 2000), to
49 archaeological and pedological surveys (Panissod *et al.* 1998, Dabas *et al.* 2000), to
50 architectonic material non-destructive testing (Féchant *et al.* 1997, Souffaché *et al.* 2010) and
51 to resistivity logging in dry holes (Leroux 2000, Guérin *et al.* 2002, Mwenifumbo *et al.* 2009).

52 Only very few instruments have been developed yet both by laboratories and manufacturers
53 (Shima *et al.* 1996, Kuras *et al.* 2007) but the use of this technique is increasing in
54 engineering geophysics.

55 Considering both the present abilities of the method and its potential developments,
56 we choose to improve the instrument specifications and design in order to increase
57 measurement reliability in noisy environments and for simultaneous measurements of both
58 resistivity and permittivity independent of geometrical scale. The new meter specifications are
59 described hereafter before presenting the results of two different case terrain applications.

60

61 **Instrument specifications and design**

62 The first choice to be achieved for the definition of a new resistivity meter is the
63 choice of the frequency range: It results from the balance between induction number and
64 capacitances of the poles, 100 kHz corresponding to a suitable upper limit. The second choice
65 is to reach as precise as possible phase measurements of the voltage by reference to the
66 injected current. This option not only corresponds to the logical improvement of presently
67 used apparatus but also to ability of measuring the permittivity in the low frequency range
68 (that may comprise both Maxwell-Wagner membrane polarization and water molecule
69 rotation (Tabbagh *et al.* 2009)); and thus exploring new paths for a series of environmental
70 applications. As a logical consequence of this second requirement, it is interesting to extend
71 the frequency range down to few milli Hz (mHz) to facilitate a full investigation of the
72 polarisation characteristics on laboratory samples with the same meter and galvanic contacts
73 (Okay 2011). To be able to use poles of limited surface ($4 \times 4 \text{ cm}^2$ for instance) in small
74 geometry arrays, the input capacitance down the pole itself should be as low as possible, less
75 than 1 pF. The voltage reference was managed in order to avoid the addition of a grounding
76 pole.

77 This instrument is called SECR-1 (Spectral Electrostatic Complex Resistivity-meter); its
78 electronics bloc diagram is presented in Figure 1a. The specifications of the meter are thus:
79 frequency range 2mHz – 100kHz, injection voltage between 40 and 400 V peak to peak
80 (maximum current 44 mA peak to peak), input capacitance <1pF and input electrical
81 resistance > 30 MΩ down each voltage pole, precision of the phase detection: 1 milliradians,
82 total measurement dynamic range: 18 bits with a LSB (least significant bit) at 19μV.

83 One of the original improvements, shown in Figure 1b, is the use of a coaxial link with shield
84 between each voltage pole and the first amplifier which is maintained at the same voltage as
85 the one of the pole.

86

87 **First Test on the Gallo-Roman archaeological site at Vieil-Evreux (Eure, France)**

88 The *Gisacum* religious centre is located 7 km east of the capital city of *Aulerques*
89 *Eburovices* (now Evreux in Normandy). There, inside a great hexagonal sacred polygon
90 covering 230 ha, stand a series of public buildings and temples, the dwelling and craft
91 activities being situated outside the polygon (Guyard and Lepert 1999). This site is located
92 over a great plateau where the superficial layer corresponds to flint clay. Above this clay, of
93 17 Ω.m resistivity, the archaeological remains have a variable thickness and may overpass
94 100 Ω.m in resistivity. None of the remains are today visible and only the thermal baths
95 building has been excavated. The electrical map of the area is presented in Figure 2 where all
96 substructions are clearly shown as resistive anomalies in white: walls of the Gallo-roman
97 temple (*fanum*), walls around the thermal complex (*peribola*), dwelling houses to the West
98 delimited by roads (*via*), aqueducts to the South bringing water to the thermal complex and to
99 the temple of water (*nymphaea*) (see Dabas *et al.* 2005 for a complete explanation of
100 archaeological features).

101 The test took place at the northern border of the *fanum* (outlined blue rectangle in
102 Figure 2) where the thickness of the archaeological I layer remains is around 90 cm. The test
103 compares the results obtained using a three depths multipole array called ARP© (Automatic
104 Resistivity Profiling), presented in Figure 3(a), to those obtained with the two depths
105 electrostatic MPG ('Multi Pôle Général') array, Figure 3(b).

106 The ARP© is of common use for pedological and archaeological applications (Dabas,
107 2009) it weighs 400 kg and has 8 spike wheels. The MPG was designed for manually towed
108 urban prospection (Dabas *et al.* 2000), it is made of fiber glass tubes and the poles are brass
109 plates encapsulated in a double sheet of rubber to avoid any galvanic contact, it weighs 40 kg.
110 Both arrays were pulled with a quad-bike over a grass cover and the measurement location
111 was obtained using a combination of dGPS system and a radar Doppler system that allows
112 checking the distance along the profile.

113 The test was performed in the field in three phases:

114 Survey1: Continuous measurement of apparent electrical resistivity using SECR-1
115 resistivity-meter and standard galvanic electrodes of the ARP© system towed by a
116 Quad bike. Data obtained will be further referred as Dataset1,

117 Survey2: Continuous measurement of apparent electrical resistivity using SECR-1
118 resistivity-meter and MPG capacitive poles manually pulled over the surface by the
119 operator. Data obtained will be further referred as Dataset2,

120 Survey3: Continuous measurement of apparent electrical resistivity using SECR-1
121 resistivity-meter and MPG capacitive poles towed continuously by the Quad bike.

122 Data obtained will be further referred as Dataset3,

123 All these Dataset were compared to the standard apparent electrical resistivity formerly
124 obtained over the same area either by the handheld RM15 (Geoscan Research ltd) resistivity-
125 meter (operating frequency 137 Hz) or by the ARP© continuous electrical profiling system

126 with its dedicated AFM05 resistivity-meter. AFM05 is a three channel regulated current
127 resistivity-meter, operating at 225Hz, and is optimized for continuous measurements with fast
128 settling time and for high tolerance in contact resistance and asymmetry in the impedance of
129 the poles.

130 Survey1: The first test was done in order to check if the SECR-1 reacts as a ‘standard’
131 resistivity-meter when pulled continuously. Mapping with the SECR-1 was repeated at two
132 different frequencies 122 Hz and 1 kHz. An area of 3700 m² was surveyed with parallel E-W
133 profiles running in zigzag. A mean inter-profile offset of 1.0m was adopted using a guided
134 real-time navigation system integrated in the process of data acquisition in the field computer
135 and with 0.19m mean inline measurement step. With an average velocity of 1.9 ms⁻¹, 38000
136 measurements were acquired in less than one hour.

137 SECR-1 measurements consist of 6 available data: the real and imaginary parts of
138 injection current, I_{ph} and I_{qu} , and the phase and quadrature components of the voltages for
139 each channel: V_{1ph} , V_{1qu} , V_{2ph} , V_{2qu} . From these data, the initial phase reference being
140 arbitrary, it is possible to plot the real and imaginary part of the apparent electrical resistivity
141 knowing the geometrical factors ($K1= 4.6m$ for channel ARP1 and $K2=10m$ for channel

142 ARP2), one has for example: $R(\rho_{al}) = K1 \frac{V_{1ph}I_{ph} + V_{1qu}I_{qu}}{I_{ph}^2 + I_{qu}^2}$ for the real part and

143 $Im(\rho_{al}) = K1 \frac{V_{1qu}I_{ph} - V_{1ph}I_{qu}}{I_{ph}^2 + I_{qu}^2}$ for the imaginary part.

144 However due to the resistivity and frequency ranges and in view of the comparison to
145 former acquired galvanic resistivity data, we here only consider the in-phase (real resistivity)
146 measurements. In order to get a map, data are then re-sampled along the profile at each dGPS
147 position and a 2D interpolation is performed (square mesh 0.25m x 0.25m). The data
148 (dataset1) corresponding to channel ARP1 and a frequency of 1 kHz is shown in colours in
149 Figure 4. Despite some slight positioning problems due to dGPS availability (a herringbone

150 effect is seen for some lines of acquisition especially in the northern part), the spatial
151 definition of anomalies is very good. Dataset1 was compared to data obtained manually with
152 RM15 resistivity-meter (in grey in Figure 4) in 1999 (manual acquisition in pole-pole
153 configuration with $a=0.5\text{m}$, in-line and between line spacing of $0,5\text{m}$). It is not possible to
154 compare the absolute values between these two Dataset because of the different array
155 geometries used and the time between surveys. Nevertheless the graphical superposition in a
156 GIS of the two maps, show the clear correspondence and superposition of all resistive
157 anomalies linked to the roman walls. After this first trial, we considered that the new SECR-1
158 can be used as a standard galvanic resistivity-meter.

159 We have then performed on the same day an acquisition of electrical resistivities using
160 the AFM05 and channel ARP1 and ARP2 configuration over a small part (map not shown).
161 Since, the AFM05 is calibrated with absolute resistance, it is possible to compare the
162 resistivities each other. The results are summarised in Table 1 using all raw data (area of $43 \times$
163 8 m^2 , raw data without re-sampling on a grid). Considering that the position of each of the
164 points is not identical between these two datasets - even if the area is the same-, the
165 correspondence in the absolute values is very good, in particular for channel ARP2 where the
166 apparent resistivities integrate a bigger volume. After these two tests, we conclude that the
167 SECR-1 can be used as a standard calibrated galvanic resistivity-meter.

168 Survey2: The second test was done in order to check the response of the SECR-1
169 when using electrostatic poles (MPG) in a simple situation where the system is pulled
170 manually by the operator (data acquisition in this situation is triggered by a simple time
171 interval). Due to the weight of the system, the area which was surveyed was limited (400m^2)
172 and was covered by 8 parallel profiles 1 m apart. Distance between points is around 8cm
173 along the profiles. The derived Dataset2 results in the map shown in figure 5 both for
174 channels MPG1 and MPG 2. All features which were previously found using either manual

175 (RM15) or continuously-towed system (ARP©) were mapped again and in great details (see
176 Fig. 2 for example). This is the first time (compared to other trials with commercially
177 available electrostatic systems) that we were able to map so clearly such structures using
178 electrostatic poles.

179 We have then performed the comparison between DS2 and resistivities obtained
180 galvanically with AFM05 (see Survey 1) and using the same electrodes configuration because
181 channel ARP2 is nearly the same geometrical configuration as channel MPG1 that is a 1m
182 square array (channel ARP1 cannot be compared to any of the MPG channel). The results of
183 this statistical analysis are shown in Table 2. Considering also the results of Survey1, it is
184 clear that apparent resistivities measured by electrostatic poles and with the SECR-1 are
185 identical with those measured galvanically. SECR-1 can now be considered as a calibrated
186 electrostatic resistivity-meter.

187 Survey3: The final step was to prove that the system can also be used dynamically by
188 pulling it on the ground surface and triggering the data acquisition by measuring the distance
189 over ground surface (Doppler radar). The whole area (3350m²) was surveyed using SECR-1
190 and the MPG configuration towed by the Quad bike in 1.15hour (average speed:1.4 ms⁻¹; 15
191 cm inline steps, 1.0m inter-profile offset, input voltage set at 196.5V and frequency set at 31
192 kHz). The resulting Dataset3 was gridded to obtain the map plotted in Figure 6a superimposed
193 to an electrical map obtained previously in 2006 using the ARP© system and a RTK (Real
194 Time Kinematics) post-processing (Dabas and Favard 2004). This quality of the derived map
195 proves that this system can be used to produce maps at a quality level equivalent to that
196 obtained with the ARP© systems even if the towing speed is still low. At present, the
197 limitation in the towing speed is due to the mechanical strength of the MPG system which
198 was not designed for this purpose.

199

200 **Second test: Thickness of the different natural and anthropogenic sediments in urban**
201 **context**

202 One of the difficulties we have to face in urban environment is to identify the nature of
203 the subsoil in the presence of high resistivity changes corresponding to the pavement itself
204 (also to the foundations of the pavement) and in the presence of a great range of utility pipes
205 that carry water, gas, telephone links, etc. These generate the high GPR reflections that hide
206 the deeper structure in the ground. Plurimetric electrostatic arrays are able to deliver correct
207 response even in presence of such features (Tabbagh and Panissod 2000), thus the new
208 resistivity meter was used within the frame of a pilot test undertaken in the city of Tours
209 (Indre et Loire, France).

210 Tours is a Gallo-Roman city built in the interfluves between two rivers, the Loire and
211 its tributary, the Cher. As a reconnaissance step of a project of new tramway transportation
212 system, we were asked to recognize the electrical resistivity of the first seven metres to assess
213 the nature of both natural and anthropogenic sediments. To achieve this goal, we used
214 electrostatic arrays that were pulled in the streets (Fig.7) during the night in order to limit the
215 traffic disturbances. Wenner β configuration with four different inter-pole distances: 3m, 5m;
216 7m and 10m was applied with a 1m measurement step. This allowed drawing apparent
217 resistivity pseudo-sections which can be compared with other sources of information. For
218 example the results obtained in one of the streets (Charles Gille) are presented in Figure 8.
219 The eastern part of this street dates back to the modern epoch and is present in a 19th century
220 city plan, whereas its western part was gone through former constructions at the beginning of
221 the 20th century. Except for the remains of a huge building between 220 and 240m, the eastern
222 part is quite conductive which can be interpreted by the absence of underground
223 constructions, while the western part exhibits higher resistivity values for the top layers ,
224 extending to few metres depth, in likely relation with the preceding building cellars or

225 foundations. A 1D three layer interpretation model allows an approximate location of the
226 depth and thickness of the conductive layer corresponding to the natural alluviums and of the
227 anthropogenic remains above.

228

229 **Conclusions**

230 The two field tests presented here allowed to first compare the electrical resistivity
231 magnitude and spatial distribution obtained by SECR-1 to the ones previously measured using
232 classical galvanic techniques. The agreement between measurements acquired with the new
233 resistivity meter and galvanic electrodes are very precise, as is the agreement between low
234 frequency measurements using electrostatic poles (capacitive) and galvanic electrodes. This
235 confirms the identity of results using both methods for shallow depth applications. The second
236 test was undertaken in a disturbed urban environment where both electrical noise and
237 underground net of pipes and cables may contaminate the signal. The electrical pseudo-
238 section is in good agreement with what is known about the city street modifications at the
239 beginning of the 20th century. In these experiments the size of the electrostatic poles, the
240 aimed depths of investigation (and thus the injected current intensities), the nature of ground
241 surfaces are sufficiently different to establish the reliability of the measurements using the
242 new resistivity meter which fulfils the requirements corresponding to the diverse applications
243 of the electrostatic method in near surface geophysics.

244

245

- 247 Benderitter Y., Jolivet A., Mounir A. and Tabbagh A. 1994. Application of the electrostatic
248 quadripole to sounding in the hectometric range of depth. *Journal of Applied Geophysics* **31**,
249 1-6.
- 250 Dabas M., Camerlynck C. and Freixas i Camps P. 2000. Simultaneous use of electrostatic
251 quadrupole and GPR in urban context: Investigation of the basement of the Cathedral of
252 Girona (Catalunya, Spain), *Geophysics* **65**, 526-532; doi:10.1190/1.1444747
- 253 Dabas M. and Favard A. 2004. Fast imaging of a Romano-Celtic temple with a decimetric
254 resolution, 1ha in 2hours? *10th European Meeting of Environmental and Engineering*
255 *Geophysics*, September 6 to 9, Utrecht.
- 256 Dabas M., Guyard L. and Lepert T. 2005. Gisacum revisité : croisement géophysique et
257 archéologie. In « *Géophysique et archéologie* », *Dossiers de l'Archéologie* **308**, 52-61.
- 258 Dabas M. 2009. Theory and practice of the new fast electrical imaging system ARP©. In:
259 *Seeing the Unseen, Geophysics and Landscape Archaeology* (Campana and Piro Ed), CRC
260 Press, 105-126.
- 261 Féchant C., Bertrand J., Mechler P. and Souffaché B. 1997. Mesure de la résistance
262 mécanique de pierres de taille in-situ. *Revue d'Archéométrie* **21**, 45-53.
- 263 Grard R. and Tabbagh A. 1991. A mobile four-electrode array and its application to the
264 electrical survey of planetary grounds at shallow depths. *J.G.R* **96**, B-3, 4117-4123.
- 265 Guérin R., Bégassat P., Benderitter Y., David J., Tabbagh A and Thiry M. 2002. Electrical
266 resistivity measurements by electromagnetic slingram mapping, electrical 2D and 3D
267 imaging, and electrostatic logging: a tool for studying an old waste landfill. *8th annual*
268 *meeting of the Environmental and Engineering Geophysical Society - European Section*,
269 *Aveiro (Portugal), 08-12/09/2002*.

270 Guyard, L. and Lepert T. 1999. Le Vieil- Evreux, ville sanctuaire gallo-romaine, *Archeologia*
271 **359**, 20-29.

272 Kuras O., Beamish D., Meldrum P. I., and Ogilvy R. D., 2006, Fundamentals of capacitive
273 resistivity technique. *Geophysics* **71-3**, 135-152.

274 Kuras O., Meldrum P. I., Beamish D., Ogilvy R. D. and Lala D. 2007. Capacitive Resistivity
275 imaging with towed arrays, *Journal of Environmental and Engineering Geophysics* **12-3**, 267-
276 279.

277 Leroux V. 2000. Utilisation d'électrodes capacitives pour la prospection électrique en forage,
278 *Thèse, Université de Rennes I*, 210 pages.

279 Mwenifumbo C. J., Barrash W., and Knoll M. D. 2009. Capacitive conductivity logging and
280 electrical stratigraphy in a high-resitivity aquifer, Boise Hydrogeophysical Research Site.
281 *Geophysics* **74-3**, E125-E133.

282 Okay G. 2011. Caractérisation des hétérogénéités texturales et hydriques des géomatériaux
283 argileux par la méthode de Polarisation Provoquée: Application à la station expérimentale de
284 Tournemire. *Thèse Université Pierre et marie Curie*, 342 pages.

285 Panissod C., Dabas M., Hesse A., Jolivet A., Tabbagh J. and Tabbagh A. 1998. Recent
286 developments in shallow electrical and electrostatic prospecting using mobile arrays.
287 *Geophysics* **63-5**, 1542-1550.

288 Shima H., Sakashita S. and Kobayashi T. 1996. Development of non-contact data acquisition
289 techniques in electrical and electromagnetic explorations. *Journal of Applied Geophysics* **35**,
290 167-173.

291 Souffaché B., Cosenza P., Flageul S., Pencole J. P., Seladji S. and Tabbagh A., 2010,
292 Electrostatic multipole for electrical resistivity measurements at decimetric scale., *Journal of*
293 *Applied Geophysics* **71-1** :6-12.

294 Tabbagh A., Cosenza P., Ghorbani A., Guérin R. and Florsch N., 2009, Modelling of
295 Maxwell-Wagner Induced Polarisation Amplitude for Clayey Materials, *Journal of Applied*
296 *geophysics* **67-2**, 109-113.

297 Tabbagh A., Hesse A. and Grard R. 1993. Determination of electrical properties of the ground
298 shallow depth with an electrostatic quadrupole: field trials on archaeological sites.
299 *Geophysical Prospecting* **41-4**, 579-597.

300 Tabbagh A. and Panissod C. 2000. 1D complete calculation for electrostatic soundings
301 interpretation. *Geophysical Prospecting* **48-3**, 511-520.

302

303

304 **Figure captions**

305 **Figure 1:** (a) Bloc diagram of the electronics of SECR-1 resistivity-meter, (b) bloc diagram of
306 the measurement channel electronics (DAC means Digital Analogic Converter, ADC means
307 Analogic Digital Converter, HV means High Voltage).

308 **Figure 2:** General apparent resistivity map of the western part of Vieil-Evreux Gallo-roman
309 site, obtained with ARP© channel 2 at 225 Hz where the experiment area corresponds to the
310 rectangle in blue

311 **Figure 3:** (a) ARP(c) system and array geometry (b) MPG system and array geometry.

312 **Figure 4:** Comparison between the apparent resistivity maps acquired using RM15 in grey
313 scale (Top of the figure, pole-pole 50cm array configuration) and Dataset1 in colour scale
314 (bottom of the figure, SECR-1 at 1kHz; channel ARP1 configuration), together with the
315 corresponding apparent resistivity histograms, values in $\Omega.m$.

316 **Figure5:** Map of Dataset2 in colour scale (SECR-1 at 31 kHz; channels MPG1 and MPG2;
317 manual measurements) with apparent resistivity histograms (values in $\Omega.m$).

318 **Figure 6:** Comparison between the apparent resistivity map acquired using AFM05 in grey-
319 scale (225 Hz; channel ARP2, continuous measurements) and Dataset3 (SECR-1 at 31 kHz;
320 channel MPG1, continuous measurements) in colour scale, together with the corresponding
321 apparent resistivity histograms (values in $\Omega.m$).

322 **Figure 7:** Sliding independent pole array (MPI, Multi-Pôles Indépendants) at the ‘nationale’
323 street in Tours (37, France).

324 **Figure 8:** (a) Pseudo section of apparent resistivity acquired using the SECR-1 at 15 kHz
325 using 3m, 5m, 7m and 10m inter-pole distances along ‘Charles Gille’ street, (b) 1D three layer
326 smoothed interpretation, and corresponding information elements (c) and (d). The natural
327 alluvium corresponds to silty sand, at 120m is located the eastern limit of ancient (modern

328 epoch) constructions, the low resistive zone between 120 and 140m can be interpreted as an
329 ancient river arm.

330

331
332

333 **Table captions**

334 **Table 1:** Dataset1: Statistics between apparent electrical resistivity ($\Omega.m$) measured with
335 AFM05 (ARP© system, at 225 Hz) and SECR-1 resistivity-meter (at 122 Hz): (N number of
336 measurements, Q1 first quartile e.g. number below which lies 25% of the data, Q3 third
337 quartile i.e. number below which lies 75% of the data).

338

339 **Table2:** Dataset2: Statistics between apparent resistivity measured with galvanic coupling and
340 apparent resistivity measured with electrostatic (capacitive) coupling.

341

342

Apparent electrical resistivity	N	Q1	Mean	Median	Q3
with AFM05 Channel1	5338	54.8	61.1	59.8	65.9
with SECR-1 Channel 1	5338	52.8	65.7	63.0	70.5
with AFM05 Channel 2	5244	44.8	51.7	49.4	55.9
with SECR-1 Channel 2	5372	43.6	51.4	48.5	55.3

343 Table 1

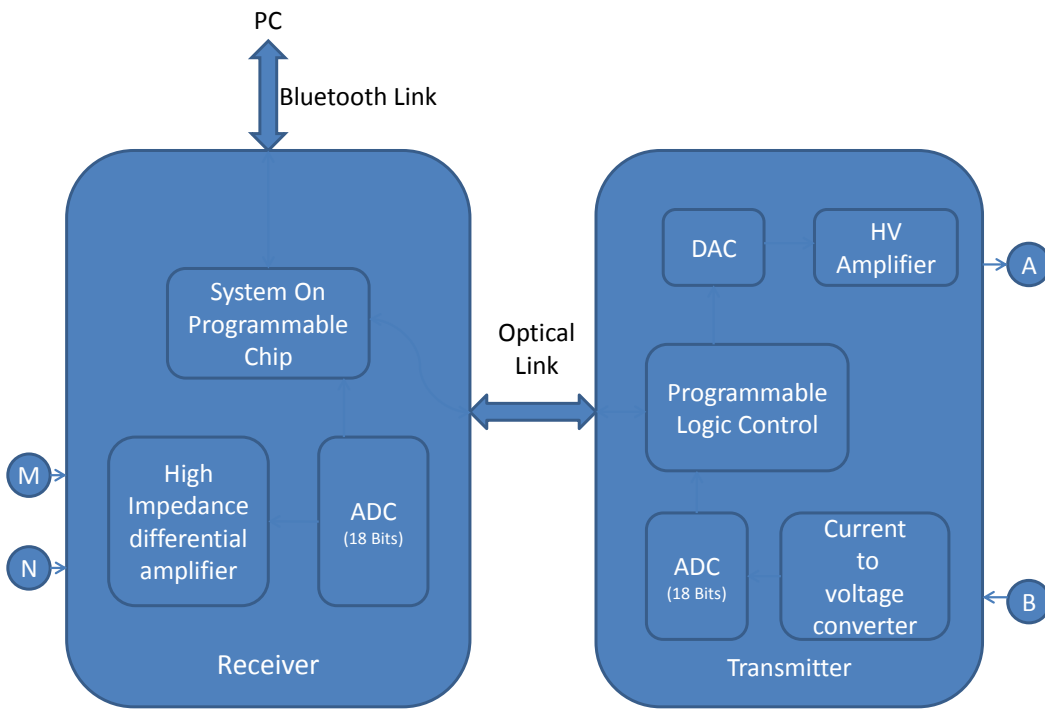
344

Apparent electrical resistivity	N	Q1	Mean	Median	Q3
ARP© channel2	3134	42.8	50.8	48.2	54.4
MGP channel 1	3134	42.6	47.9	46.3	51.1

345 Table 2

346

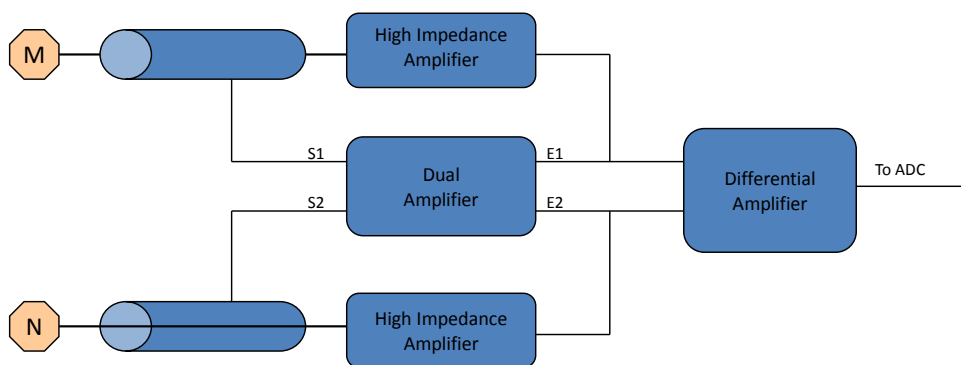
347



348

Fig: 1(a)

349



350

Fig1(b)

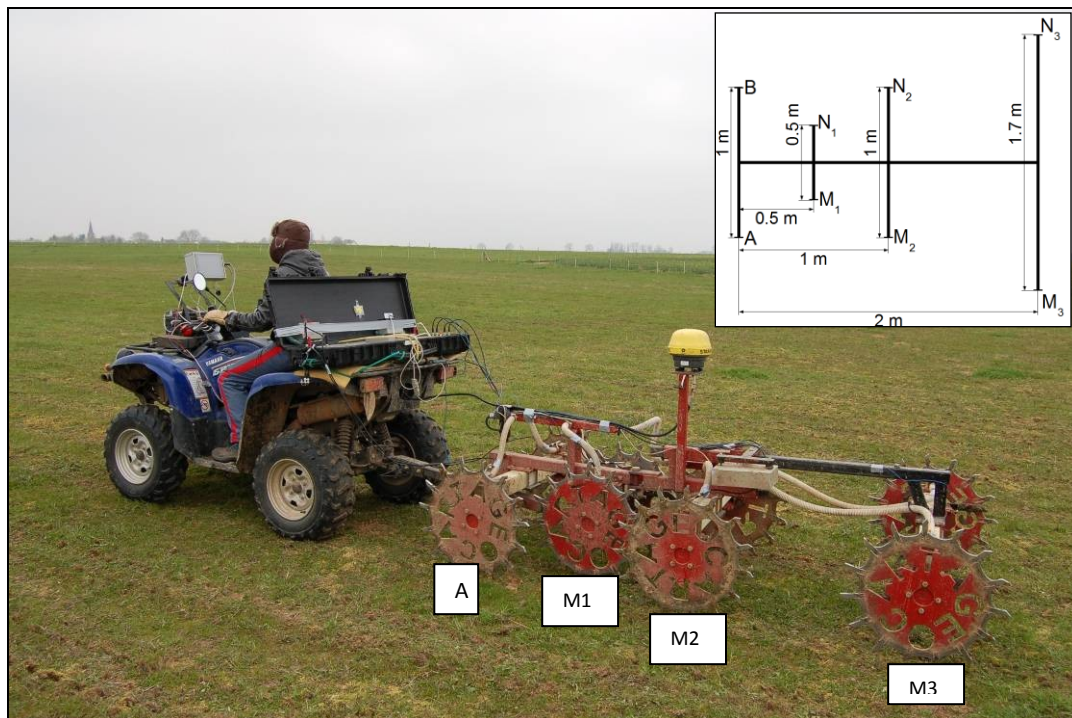
351



352

353 Fig 2

354 Fig. 3(a)



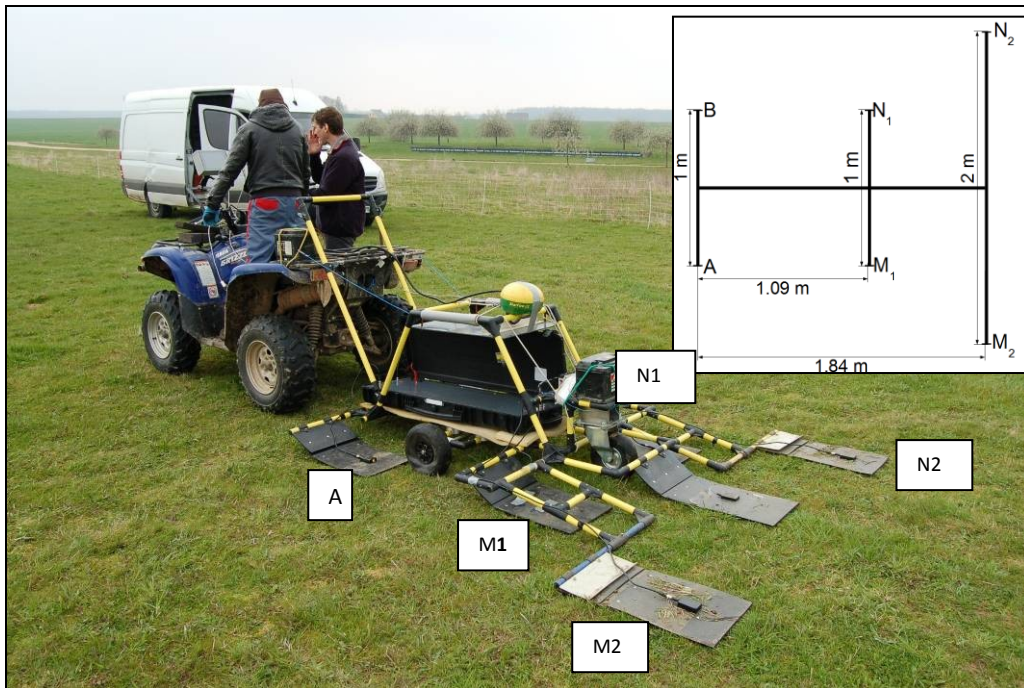
355

356

357

358

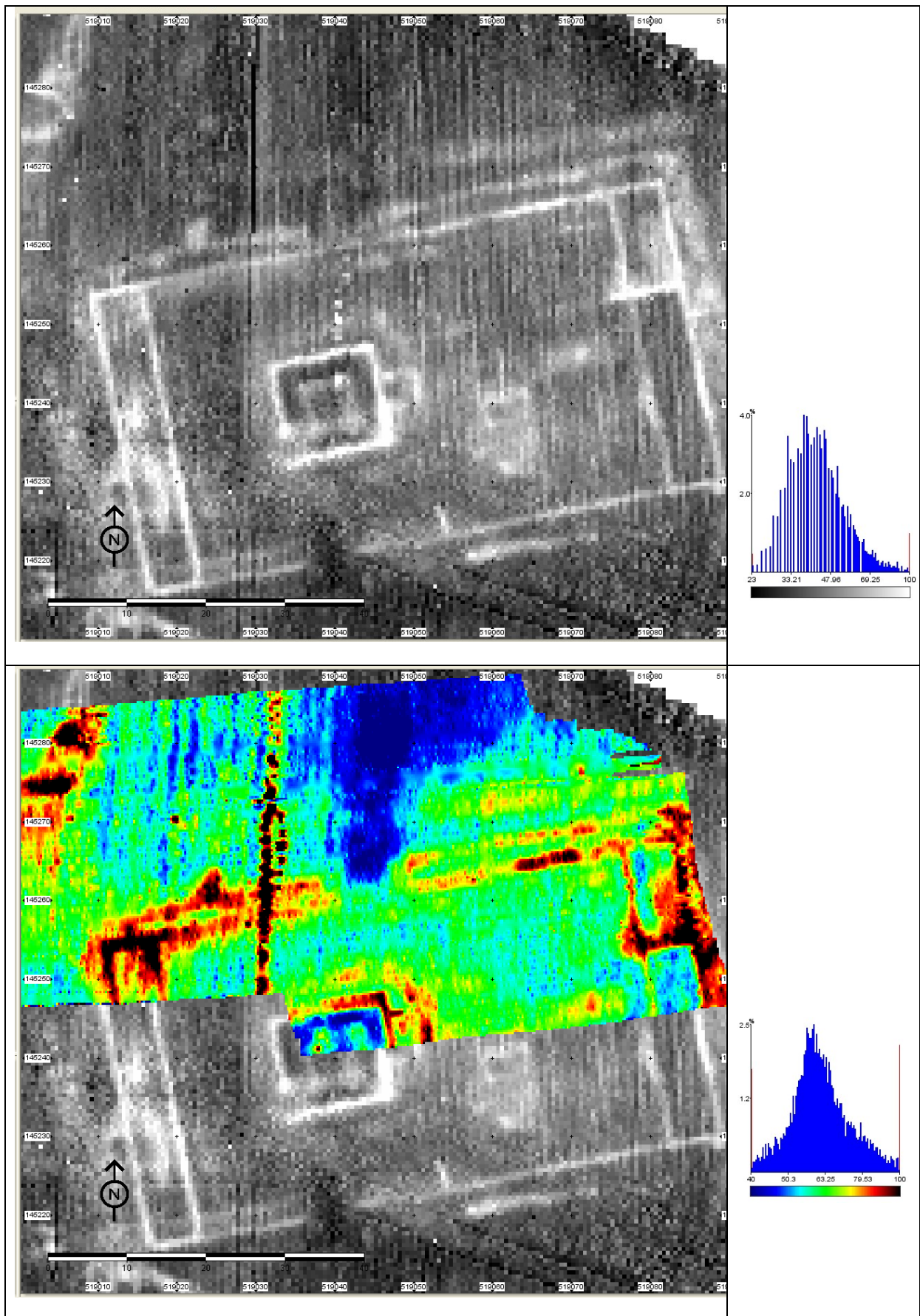
359 Fig3 (b)



360

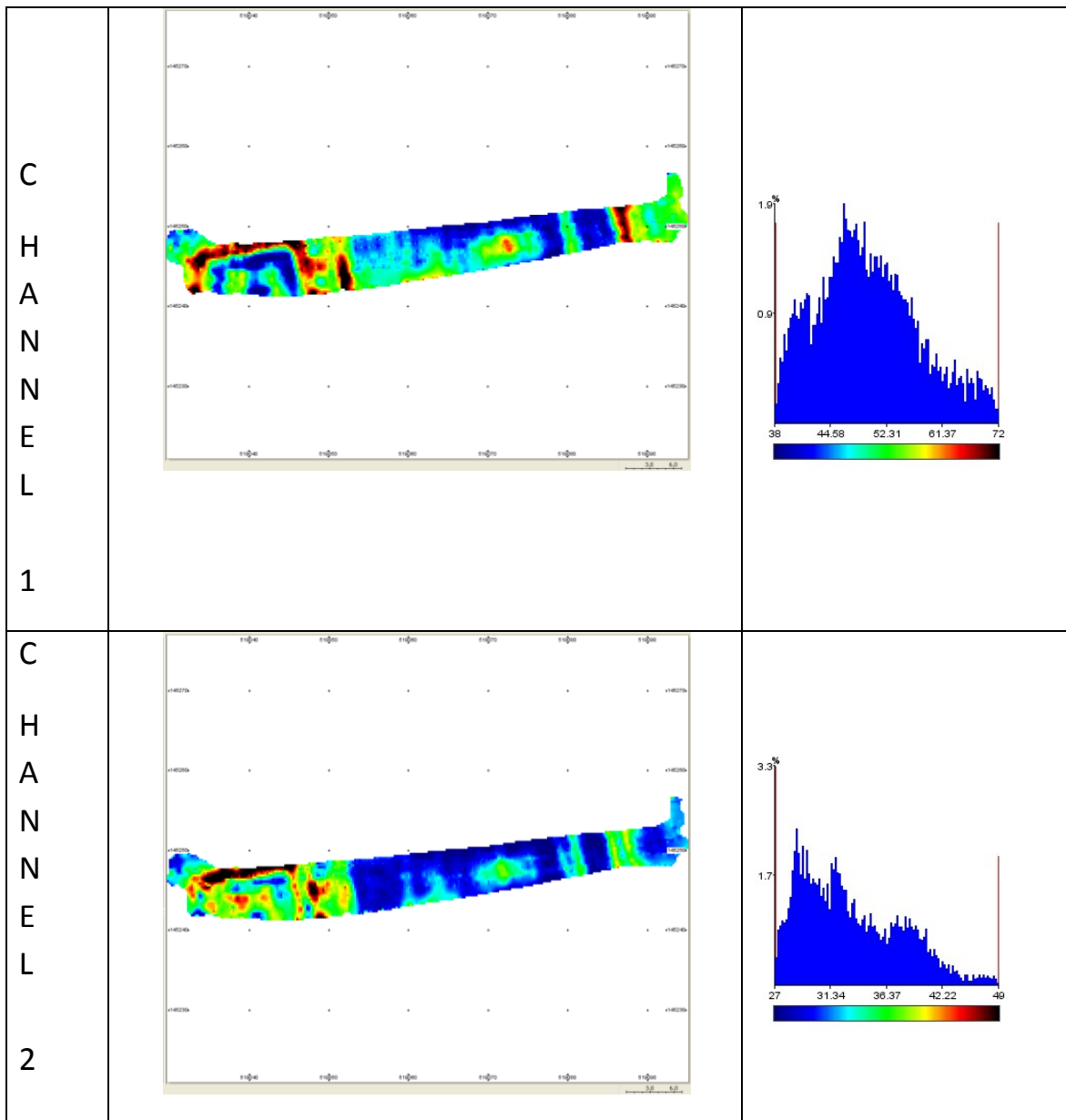
361

362 Fig4



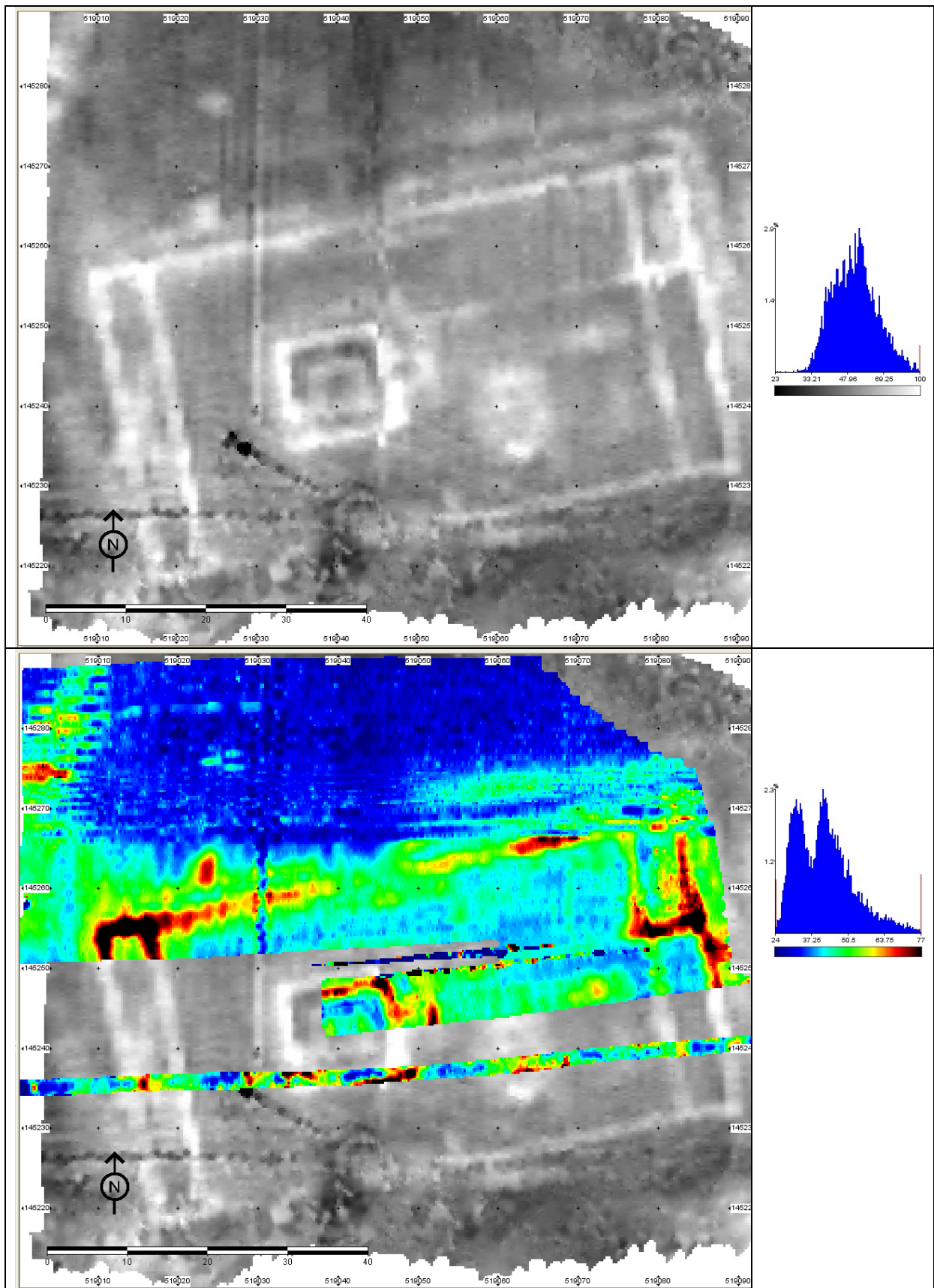
363

364 Fig 5

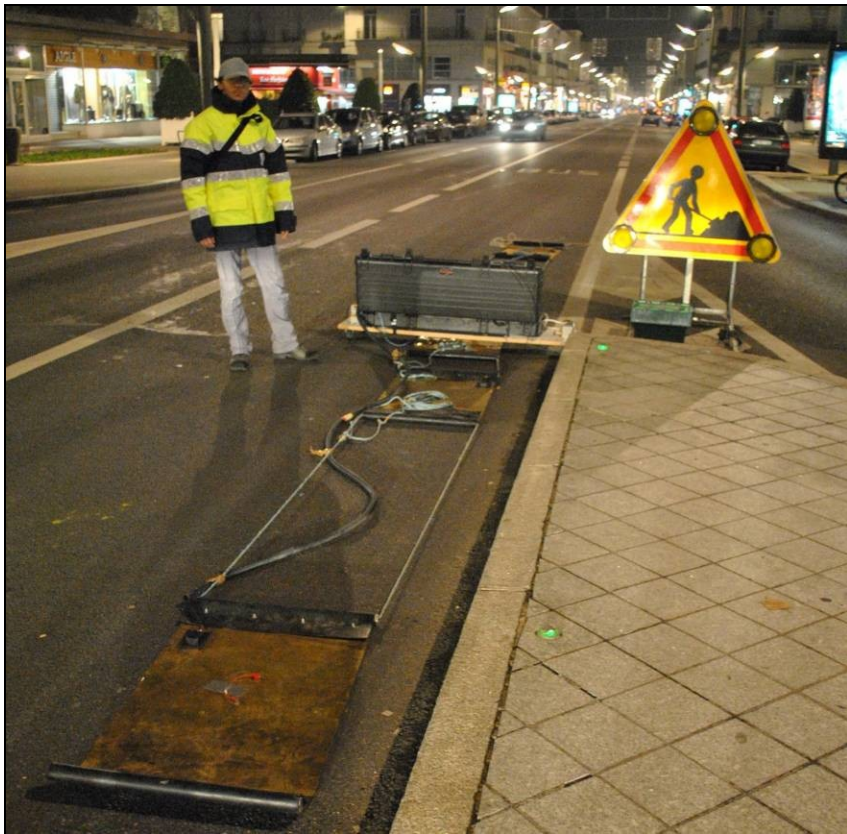


365

366



369 Fig. 7



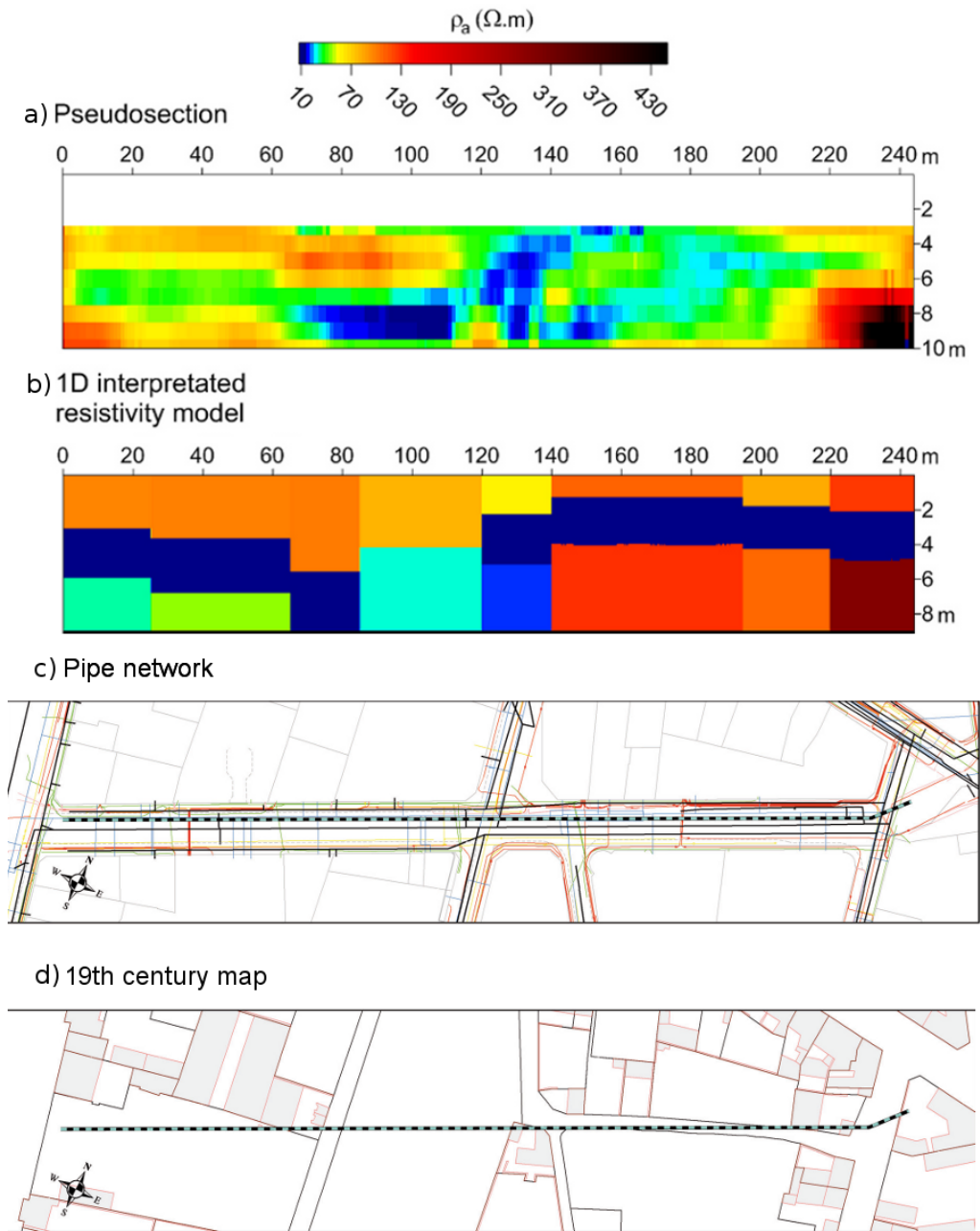
370

371

372

373

374 Fig. 8



375